ISCI, Volume *4*

Supplemental Information

Human Organ-Specific

Endothelial Cell Heterogeneity

Raluca Marcu, Yoon Jung Choi, Jun Xue, Chelsea L. Fortin, Yuliang Wang, Ryan J. Nagao, Jin Xu, James W. MacDonald, Theo K. Bammler, Charles E. Murry, Kimberly Muczynski, Kelly R. Stevens, Jonathan Himmelfarb, Stephen M. Schwartz, and Ying Zheng

Transparent Methods

Isolation and culture of organ specific endothelial cells. All experiments were approved by the Institutional Review Board of the University of Washington (IRB447773EA). Normal human fetal organs were obtained upon informed consent from abortion material (age 16-20 weeks) and the same donor tissues (kidney, lung, liver, and heart) were used to isolate organ specific endothelial cells. Tissues were minced finely in serum-free EBM-2 endothelial growth medium (Lonza) supplemented with 0.2 mg/ml Liberase and 100 U/ml DNase (Roche) and incubated for 30 min at 37 ^{0}C in a water bath with shaking. The resulting tissue homogenate was filtered twice through a 40 μm cell strainer to remove tissue debris and large vessels. For the isolation of fresh endothelial cells, EpCAM-positive cells were depleted first from the cell suspension using EpCAM microbeads (Miltenyi Biotec), followed by the depletion of CD45-positive cells using CD45 MicroBeads (Miltenyi Biotec). Then the CD144 positive cells were magnetically separated using CD144 MicroBeads (Miltenyi Biotec) on 2 different columns. For cultured endothelial cells, the cell suspension was plated on gelatin coated T-75 flasks in EBM-2 medium supplemented with antibiotic/antimycotic (Invitrogen), 10% FBS (Invitrogen), 100 μg/ml ECGS (Millipore), 50 μg/ml Heparin (Invitrogen), and 40 ng/ml VEGF (R&D Systems). For kidney and lung samples, epithelial cells were removed from the cell suspension before plating using EpCAM microbeads (Miltenyi Biotec) to prevent epithelial cell overgrowth. Cells were cultured at 5% O_2 until confluent and then endothelial cells as the CD144 positive and CD45 negative population were sorted on BD FACSAria II at the UW SLU Flow Cytometry Facility. After sorting, organ specific endothelial cells were cultured in EBM-2 supplemented with antibiotic/antimycotic, 10% FBS, 100 μg/ml ECGS, 50 μg/ml Heparin, and 20 ng/mL VEGF, on gelatin-coated plates and used for further experiments between passages 1-3.

Histology. Human fetal organs (kidney, lung, liver and heart) were embedded in Tissue-Tek O.C.T. compound (Sakura) and kept as frozen blocks at -80 ^{0}C. Frozen organ sections were cut to a thickness of 9 μm using a cryostat (Leica CM 1850) and placed on HistoBond adhesive glass slides (Marienfeld). The glass slides were air-dried for 30 min

and fixed in 4% formaldehyde. Fixed tissues were stained with hematoxylin and eosin (H&E).

Immunofluorescence. Tissue cryosections and organ specific endothelial cells plated on gelatin-coated glass slides were fixed with 3.7% formaldehyde, permeabilized with 2% BSA and 0.5% Triton x-100 in PBS, blocked with Background Buster (Innovexbio), and incubated overnight at 4 ^{0}C with primary antibodies against CD31 (Life Technologeis), CD144 (Abcam), PLVAP (Abcam), Caveolin-1 (Abcam), vWF (Abcam), ART4 (Bioss Inc), TBX5 (Santa Cruz Biotechnology), HNF1B (Abnova), and KCNJ16 (LSBio), followed by Alexa-488, -568, or -647 secondary antibodies (Invitrogen) and Hoechst (Life Technologies) staining. Cells were imaged with a Nikon Confocal microscope or Nikon wide filed microscope using 20X and 40X objectives. Image analysis was performed using the Image J software (U.S. National Institute of Health, Bethesda, Maryland).

Flow cytometry analysis. To characterize single endothelial cell populations within each fetal organ, multiparameter FACS analysis of stained organ suspensions was performed on a BD FACSCanto II and quantitated with FlowJo software (Tree Star). The following antibodies were used: APC-anti-CD144 (eBioscience), FITC-anti-CD31 (BD Biosciences), Pacific Blue-anti-CD45 (BioLegend), FITC-anti-CD34 (BD Biosciences), PE-anti-EphB4 (R&D systems), FITC-anti-gp38 (R&D systems), FITC-anti-Robo1 (R&D system), PE-anti-CD144 (BioLegend), APC-anti-PDGFRβ (BioLegend), PE-anti-EpCAM(Miltenyi Biotec), PE-anti-α-SMA (R&D systems) and FITC-anti-NG2 (R&D systems). Unstained controls, single stained cellular controls, and single stained BD™ CompBead particles were used for compensation and voltage adjustment. Isotype control antibodies were used to distinguish non-specific background signals from specific signals.

RNA isolation, RNA sequencing and RT-PCR. Total RNA from cultured and freshly isolated organ specific endothelial cells was purified using the RNAeasy Mini Kit (Qiagen) and residual DNA was removed by on-column DNase digestion. RNA quality was assessed with the Agilent RNA 6000 Nano Kit using the Agilent 2100 Bioanalyzer

(Agilent Technologies). Only samples with RNA integrity number higher than 8 were kept for further analysis. RNA sequencing was performed on poly-A-enriched samples using Illumina TruSeq. RT-PCR was performed using the Real-time PCR System (Applied Biosystems) with Fast SYBR Green Master Mix (Applied Biosystems). The abundance of each gene was determined relative to an internal control using GAPDH RNA.

RNA-seq data analysis. RNA-seq samples were aligned to hg19 using Tophat (Trapnell et al., 2009). Gene-level read counts were quantified using htseq-count (Anders et al., 2015) using Ensembl GRCh37 gene annotations. Genes with total expression above 10 normalized read counts summed across RNA-seq samples were kept for further analysis. princomp function from R was used to for Principal Component Analysis. DESeq (Anders and Huber, 2010) was used for differential gene expression analysis. Genes with fold change >1.5 and FDR<0.05 were considered differentially expressed. topGO R package (Alexa et al., 2006) was used for Gene Ontology enrichment analysis. The gene expression data set has been submitted to the public database in Gene Expression Omnibus.

Western blot analysis. Cells and tissues were lysed in RIPA buffer (Sigma) supplemented with protease inhibitor cocktail (Thermo Scientific). 3 μg proteins were electrophoresed on NuPAGE 4-12% Bis-Tris Acrilamide gels (Invitrogen), transferred on PVDF membrane and probed overnight at 4°C with primary antibodies against Von Willebrand Factor (Abcam), caveolin (Abcam), PV1 (Abcam) and GAPDH (Cell Signaling). HRP-conjugated secondary antibodies (Thermo Scientific) were used for detection.

Endothelial barrier function measurements. The EC barrier function was evaluated by real-time measurements of electrical impedance with the xCELLigence RTCA SP instrumentation (ACEA Bioscience, Inc.). Organ specific endothelial cells were plated in a 96-well electronic microtiter plates (E-Plate 96, ACEA Bioscience, Inc.), 10,000 cells/well, and allowed to reach cellular confluence, as indicated by plateau values obtained for the electrical impedance (60-68 hours). At plateau, the electrical impedance

readout expressed in arbitrary units as the Cell index parameter, reflects changes in barrier function and permeability of different endothelial cells.

Spheroid sprouting assay. Endothelial spheroids containing 1000 cells/spheroid were generated using the "hanging drop" technique in endothelial growth medium with 20% Methocel solution (2% Methyl cellulose (Sigma) in EBM2 growth medium). Spheroids were plated into 24 well plates, 40 spheroids/well, embedded in 2 mg/ml type I collagen and 30% Methocel matrix, overlaid with endothelial growth medium supplemented with 40 ng/ml VEGF. Spheroids were allowed to sprout for 24-48 hours and imaged using a 10x objective. Sprouts number and length were quantified using the Image J software (U.S. National Institute of Health, Bethesda, Maryland).

Fabrication of vascular networks. Three-dimensional, perfusable vascular networks were fabricated as described previously(Zheng et al., 2012). Briefly, microvessels were fabricated by seeding organ specific endothelial cells in microfluidic channels embedded in 6.5 mg/ml type I collagen matrix. The networks were cultured with gravity-driven flow of endothelial growth medium for 5 days, fixed and employed for either electron microscopy or confocal microscopy imaging.

Transmission electron microscopy. Microfluidic vascular networks were fixed by perfusion in 2.5% glutaraldehyde for 20 min followed by immersion in half-strength Karnovsky's solution (2% paraformaldehyde/2.5% glutaraldehyde in 0.2M cacodylate buffer) for 4 hr. These samples were rinsed in 0.1M cacodylate buffer then post-fixed using 2% OsO4 in 0.2M cacodylate buffer followed by another rinse with 0.1M cacodylate buffer. Sample dehydration was performed using immersions in graded solutions of ethanol, then propylene oxide (PO), before 1:1 PO/Epon 812 (vendor) immersion overnight. Fresh Epon 812 was then exchanged for 2 hr after which the blocks were cured for 48 hr at 60oC. Ultrathin sections (70 nm) were cut from blocks using a diamond (vendor) blade on a Leica EMUC6 ultra-microtome and placed onto grids. Grids were stained with uranyl acetate for 2 hr and lead citrate for 5 min. Sections were imaged using a JEOL JEM-1400 Transmission Electron Microscope (JEOL Ltd., Japan) using a

typical acceleration voltage around 100 kV. Images were acquired with a Gatan Ultrascan 1000XP camera (Gatan, Inc., Pleasanton, CA).

Metabolism. Oxygen consumption rate (OCR) and extracellular acidification rate (ECAR) were measured using the XF96 Seahorse Analyzer (Seahorse Bioscience). ECs were plated into 96-well Seahorse assay plates in complete growth medium, 7000 cells/well, 3 days before measurements. OCR and ECAR measurements were performed in XF Assay medium (Seahorse Bioscience), supplemented with 5 mM glucose, 1 mM sodium pyruvate and 10 mM glutamine, at 9 minutes intervals. Time course of OCR and ECAR was performed upon sequential addition of Oligomycin (1 μM), CCCP (1 μM), and Rotentone/Antimycin (1 μM each). At the end of the measurements, the protein content for each well was quantified, and OCR and ECAR values were normalized per microgram of protein for each cell type.

*Hepatocyte isolation, culture, and functional analysi*s: Hepatocytes were isolated from 100-140g adult female Lewis rats (Taconic), as described previously.(Dunn et al.) Briefly, the animals were anesthetized using isoflurane, the portal vein was cannulated with an 18G catheter, and the liver was perfused and digested with collagenase type IV (Sigma). Hepatocytes were purified via Percoll centrifugation and seeded at a density of 0.3e06 hepatocytes per well onto 24-well plates coated with 0.17 mg/ml rat tail Collagen-1 (BD Biosciences). The next day, normal human dermal fibroblasts (Lonza, ratio of 1:1) or fetal (isolated) liver, kidney, heart, lung, or human umbilical vein (Lonza) endothelial cells (ratio of 1:0.3) were seeded onto the hepatocytes. Cultures were maintained for eight days in a 1:1 mixture of “hepatocyte medium” [DMEM with high glucose (4.5g/L), 10% (v/v) fetal bovine serum (Biowest), 0.04 ug/ml dexamethasone, 7 ng/ml glucagon, 1% ITS+ culture supplement (Corning), 1.5% 1M HEPES, and 1% penicillin-streptomycin] and “endothelial medium” [EBM-2 supplemented with antibiotic/antimycotic, 10% FBS, 100 μg/ml ECGS, 50 μg/ml Heparin, and 20 ng/mL VEGF]. Culture media was collected daily from each well before replacement with fresh medium. Rat albumin in collected media was measured via enzyme-linked immunosorbent assay (Bethyl labs). After 7 days, cultures were fixed and hepatocytes were stained against pan cytokeratin (Sigma) and

endothelial cells against VE-Cad and PV-1. The immunofluorescence images were taken in Nikon wide filed microscope using 20X and 40X objectives.

References

Alexa, A., Rahnenfuhrer, J., and Lengauer, T. (2006). Improved scoring of functional groups from gene expression data by decorrelating GO graph structure. Bioinformatics *22*, 1600-1607.

Anders, S., and Huber, W. (2010). Differential expression analysis for sequence count data. Genome Biology *11*.

Anders, S., Pyl, P.T., and Huber, W. (2015). HTSeq-a Python framework to work with high-throughput sequencing data. Bioinformatics *31*, 166-169.

Dunn, J.C., Tompkins Rg Fau - Yarmush, M.L., and Yarmush, M.L. Long-term in vitro function of adult hepatocytes in a collagen sandwich configuration.

Trapnell, C., Pachter, L., and Salzberg, S.L. (2009). TopHat: discovering splice junctions with RNA-Seq. Bioinformatics *25*, 1105-1111.

Zheng, Y., Chen, J., Craven, M., Choi, N., Totorica, S., Diaz-Santana, A., Kermani, P., Hempstead, B., Fischbach-Teschl, C., Lopez, J.A., *et al.* (2012). In vitro microvessels for the study of angiogenesis and thrombosis. Proceedings of the National Academy of Sciences of the United States of America *109*, 9342-9347.

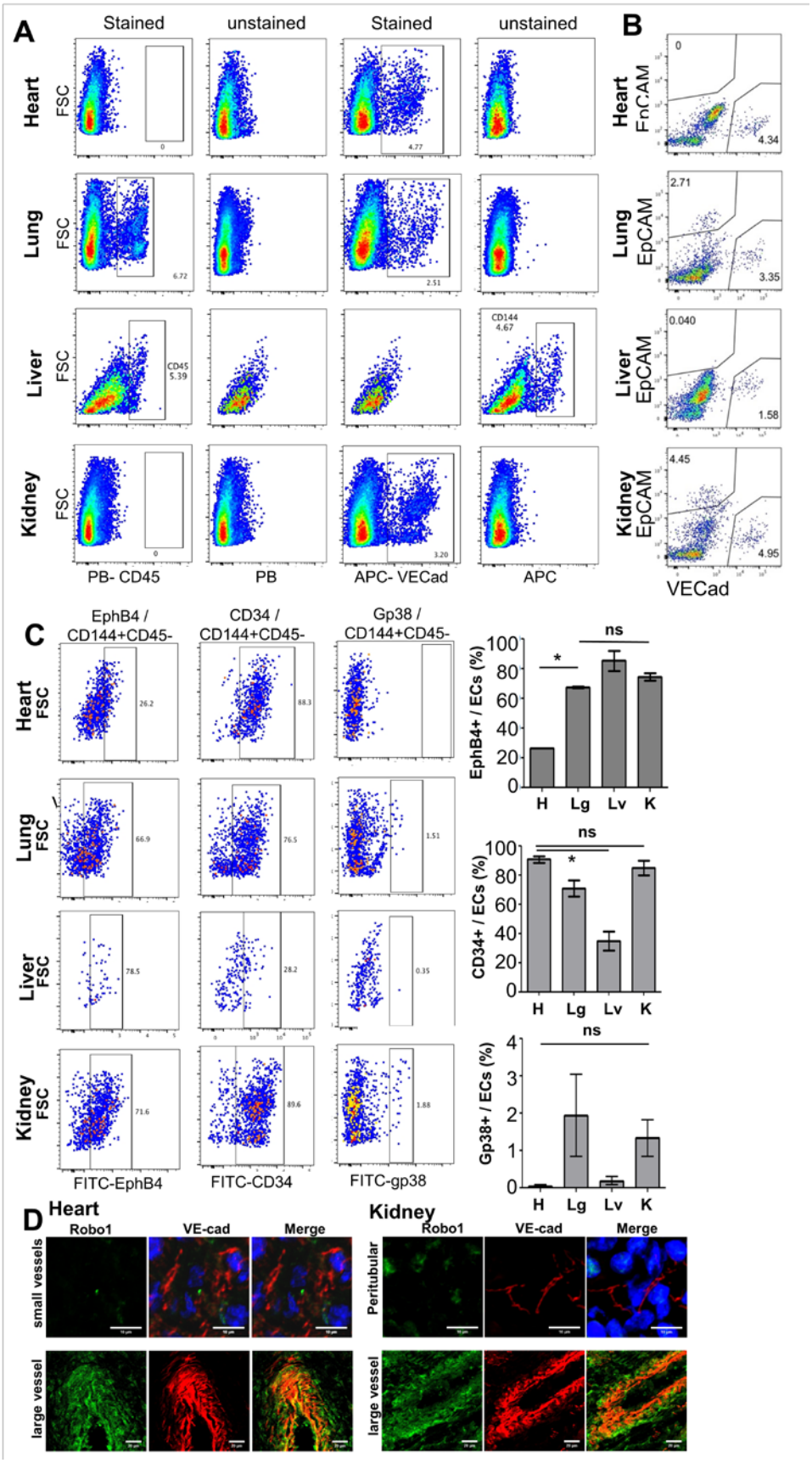
A
Stained
unstained
Stained
unstained
Heart
Lung
Liver
Kidney
FSC
CD45
5.39
CD144
4.67
PB- CD45
PB
APC- VECad
APC
B
Heart
FnCAM
Lung
EpCAM
Liver
EpCAM
Kidney
EpCAM
VECad
C
EphB4 /
CD144+CD45-
CD34 /
CD144+CD45-
Gp38 /
CD144+CD45-
FITC-EphB4
FITC-CD34
FITC-gp38
EphB4+ / ECs (%)
CD34+ / ECs (%)
Gp38+ / ECs (%)
H
Lg
Lv
K
ns
D
Heart
Kidney
Robo1
VE-cad
Merge
small vessels
large vessel
Peritubular

Fig. S1, related to Fig. 1. Characterization of cell population in human fetal tissue. A-B. Representative flow cytometry profiles of fresh total cell tissue suspension from fetal human heart, lung, liver and kidney stained with antibodies (A) against CD45 and CD144 (VECad), in comparison with unstained controls, and (B) VECad amd EpCam. **C.** Flow cytometry analysis of EC population in fresh fetal tissue for EphB4+, CD34+, and Gp38+ with quantification for three donor sets. **D**. Representative immunofluorescence images of small vessels and large vessels in frozen heart and kidney tissue sections stained with antibodies against Robo1 and VECad.

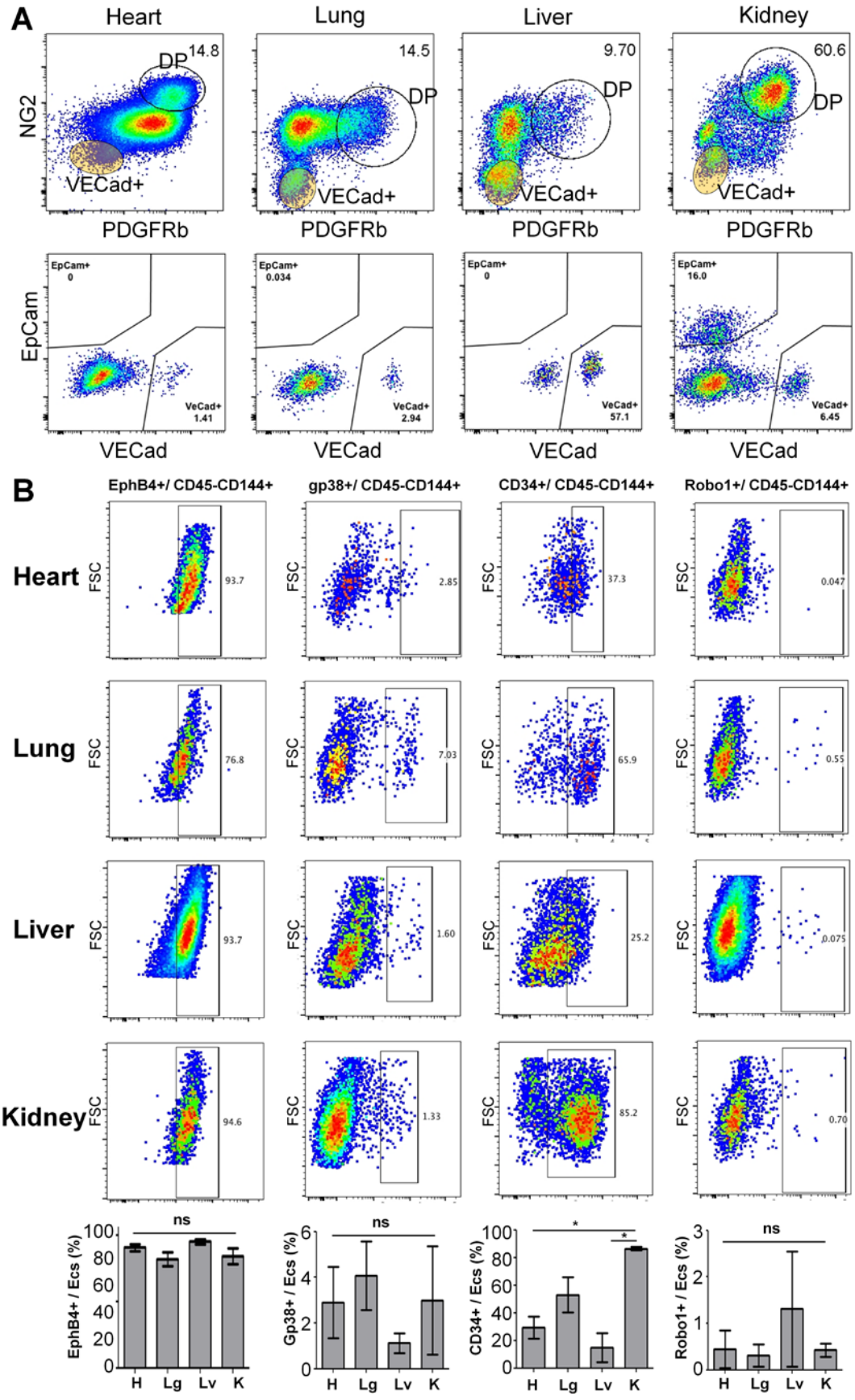
A
Heart
Lung
Liver
Kidney
NG2
PDGFRb
DP
VECad+
14.8
14.5
9.70
60.6
EpCam
VECad
EpCam+ 0
EpCam+ 0.034
EpCam+ 0
EpCam+ 16.0
VeCad+ 1.41
VeCad+ 2.94
VeCad+ 57.1
VeCad+ 6.45
B
EphB4+/ CD45-CD144+
gp38+/ CD45-CD144+
CD34+/ CD45-CD144+
Robo1+/ CD45-CD144+
Heart
Lung
Liver
Kidney
FSC
93.7
2.85
37.3
0.047
76.8
7.03
65.9
0.55
93.7
1.60
25.2
0.075
94.6
1.33
85.2
0.70
EphB4+ / Ecs (%)
Gp38+ / Ecs (%)
CD34+ / Ecs (%)
Robo1+ / Ecs (%)
ns
*
H
Lg
Lv
K

Fig. S2, related to Fig. 2. Analysis of enriched cell suspension. A. Representative flow cytometry and sorting profiles of enriched cell suspension from fetal human heart, lung, liver and kidney, stained with antibodies against NG2 and PDGFRb, with VECad+ population from Fig.2A marked as orange circles. B. Flow cytometry analysis of cultured human heart, lung, liver, and kidney EC populations for EphB4+, Gp38+, CD34+ and Robo1+.

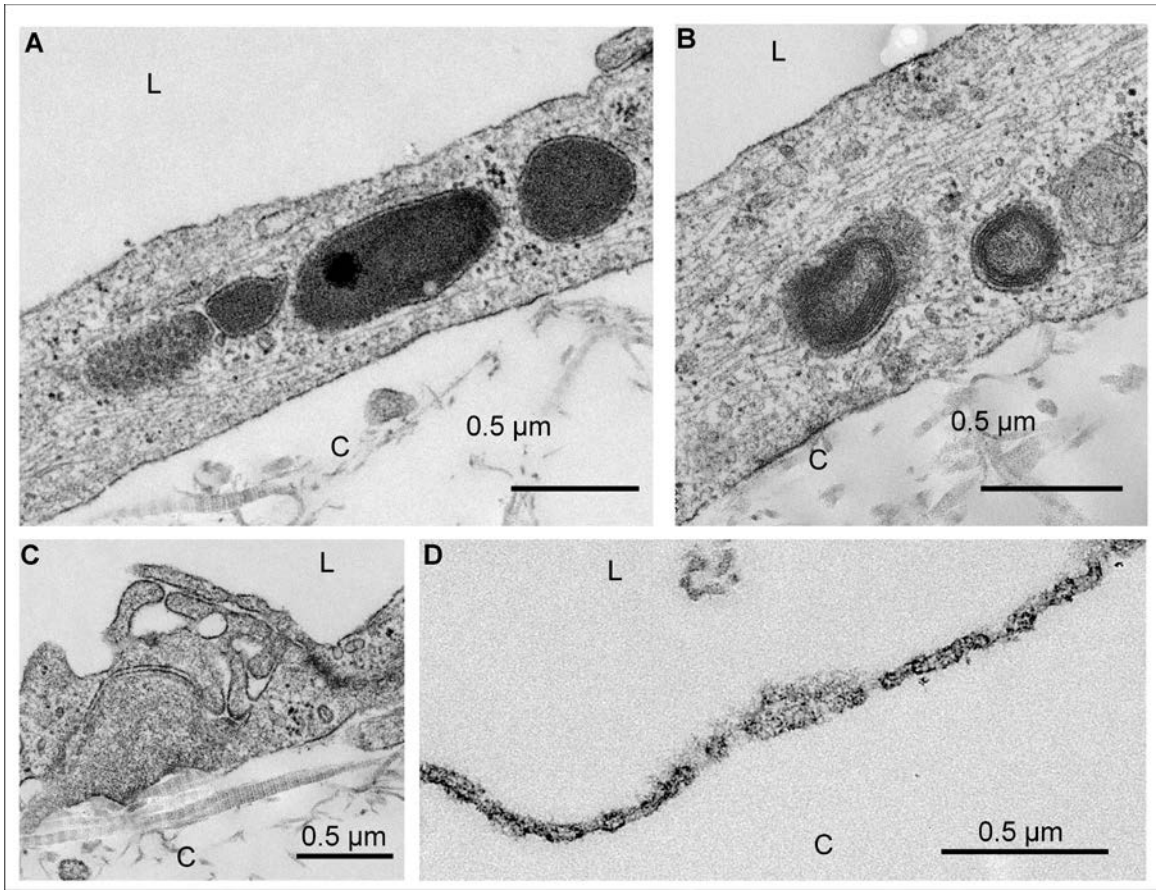

Fig. S3, related to Fig. 3. Ultrastructural images of human fetal liver ECs. A-B. Ultrastructural images of multivascular bodies, lysosomes, and other intracellular features in liver ECs. C-D. Sinusoidal and fenestrated features on liver EC membranes.

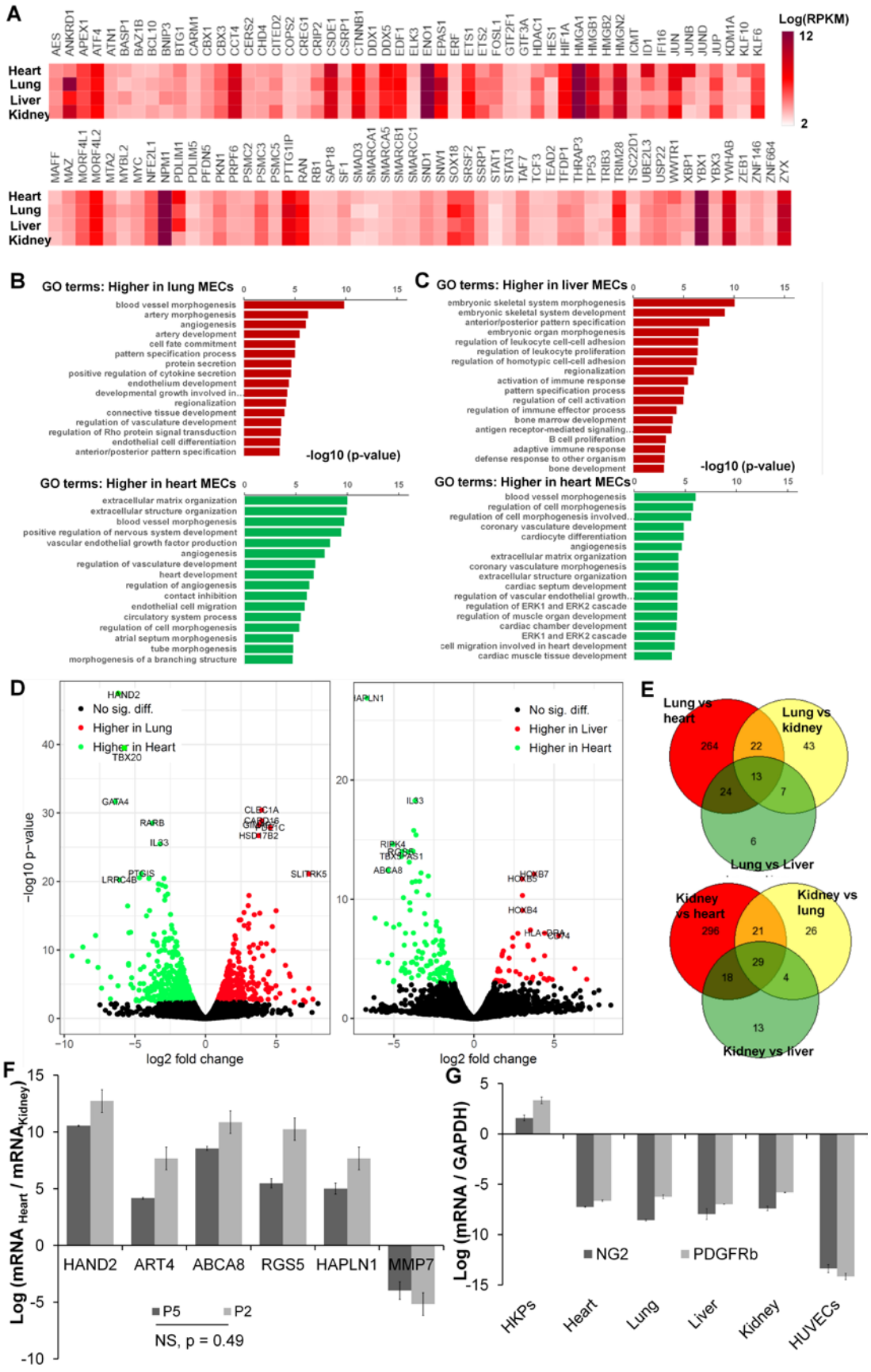
A
Log(RPKM)
12
2
Heart
Lung
Liver
Kidney
AES ANKRD1 APEX1 ATF4 ATN1 BASP1 BAZ1B BCL10 BNIP3 BTG1 CARM1 CBX1 CBX3 CCT4 CERS2 CHD4 CITED2 COPS2 CREG1 CRIP2 CSDE1 CSRP1 CTNNB1 DDX1 DDX5 EDF1 ELK3 ENO1 EPAS1 ERF ETS1 ETS2 FOSL1 GTF2F1 GTF3A HDAC1 HES1 HIF1A HMGA1 HMGB1 HMGB2 HMGN2 ICMT ID1 IFI16 JUN JUNB JUND JUP KDM1A KLF10 KLF6
MAFF MAZ MORF4L1 MORF4L2 MTA2 MYBL2 MYC NFE2L1 NPM1 PDLIM1 PDLIM5 PFDN5 PKN1 PRPF6 PSMC2 PSMC3 PSMC5 PTTG1IP RAN RB1 SAP18 SF1 SMAD3 SMARCA1 SMARCA5 SMARCB1 SMARCC1 SND1 SNW1 SOX18 SRSF2 SSRP1 STAT1 STAT3 TAF7 TCF3 TEAD2 TFDP1 THRAP3 TP53 TRIB3 TRIM28 TSC22D1 UBE2L3 USP22 WWTR1 XBP1 YBX1 YBX3 YWHAB ZEB1 ZNF146 ZNF664 ZYX
B
GO terms: Higher in lung MECs
blood vessel morphogenesis
artery morphogenesis
angiogenesis
artery development
cell fate commitment
pattern specification process
protein secretion
positive regulation of cytokine secretion
endothelium development
developmental growth involved in...
regionalization
connective tissue development
regulation of vasculature development
regulation of Rho protein signal transduction
endothelial cell differentiation
anterior/posterior pattern specification
-log10 (p-value)
GO terms: Higher in heart MECs
extracellular matrix organization
extracellular structure organization
blood vessel morphogenesis
positive regulation of nervous system development
vascular endothelial growth factor production
angiogenesis
regulation of vasculature development
heart development
regulation of angiogenesis
contact inhibition
endothelial cell migration
circulatory system process
regulation of cell morphogenesis
atrial septum morphogenesis
tube morphogenesis
morphogenesis of a branching structure
C
GO terms: Higher in liver MECs
embryonic skeletal system morphogenesis
embryonic skeletal system development
anterior/posterior pattern specification
embryonic organ morphogenesis
regulation of leukocyte cell-cell adhesion
regulation of leukocyte proliferation
regulation of homotypic cell-cell adhesion
regionalization
activation of immune response
pattern specification process
regulation of cell activation
regulation of immune effector process
bone marrow development
antigen receptor-mediated signaling...
B cell proliferation
adaptive immune response
defense response to other organism
bone development
-log10 (p-value)
GO terms: Higher in heart MECs
blood vessel morphogenesis
regulation of cell morphogenesis
regulation of cell morphogenesis involved...
coronary vasculature development
cardiocyte differentiation
angiogenesis
extracellular matrix organization
coronary vasculature morphogenesis
extracellular structure organization
cardiac septum development
regulation of vascular endothelial growth...
regulation of ERK1 and ERK2 cascade
regulation of muscle organ development
cardiac chamber development
ERK1 and ERK2 cascade
cell migration involved in heart development
cardiac muscle tissue development
D
No sig. diff.
Higher in Lung
Higher in Heart
HAND2
TBX20
GATA4
RARB
IL33
PTGIS
LRRC4B
SLITRK5
−log10 p−value
log2 fold change
No sig. diff.
Higher in Liver
Higher in Heart
HAPLN1
IL33
RIPK4
RGS5
TBX3
PAS1
ABCA8
HOXB7
HOXB5
HOXB4
HLA-DRA
CD74
log2 fold change
E
Lung vs heart
Lung vs kidney
Lung vs Liver
Kidney vs heart
Kidney vs lung
Kidney vs liver
264
22
43
13
24
7
6
296
21
26
29
18
4
13
F
Log (mRNA Heart / mRNA Kidney)
HAND2
ART4
ABCA8
RGS5
HAPLN1
MMP7
P5
P2
NS, p = 0.49
G
Log (mRNA / GAPDH)
NG2
PDGFRb
HKPs
Heart
Lung
Liver
Kidney
HUVECs

Fig. S4, related to Fig. 4. Global RNA sequencing analysis for four types of human fetal ECs and gene validation. **A**. Top expressed transcripts (107 TFs) for organ-specific ECs. Colormap: log(RPKM). **B-C**. Gene Ontology terminology analysis for lung vs. heart (B) and liver vs. heart (C) differentially expressed EC genes. **D**. Volcano plots of -log10 p-value vs. log2 fold change for lung vs. heart (left), and liver vs. heart (right) differentially expressed EC genes. **E**. Venn diagram showing organ-specific, differentially expressed genes for the lung and kidney ECs. **F.** Log fold changes of selected gene expression comparing heart vs. kidney ECs at passage 2 and 5, showing no significant difference. **G.** mRNA expression of NG2 and PDGFRb comparing four isolated and cultured fetal ECs with HUVECs and human kidney pericytes (HKPs), the isolated NG2+PDGFRb+ population shown in Supplementary Fig. 2.

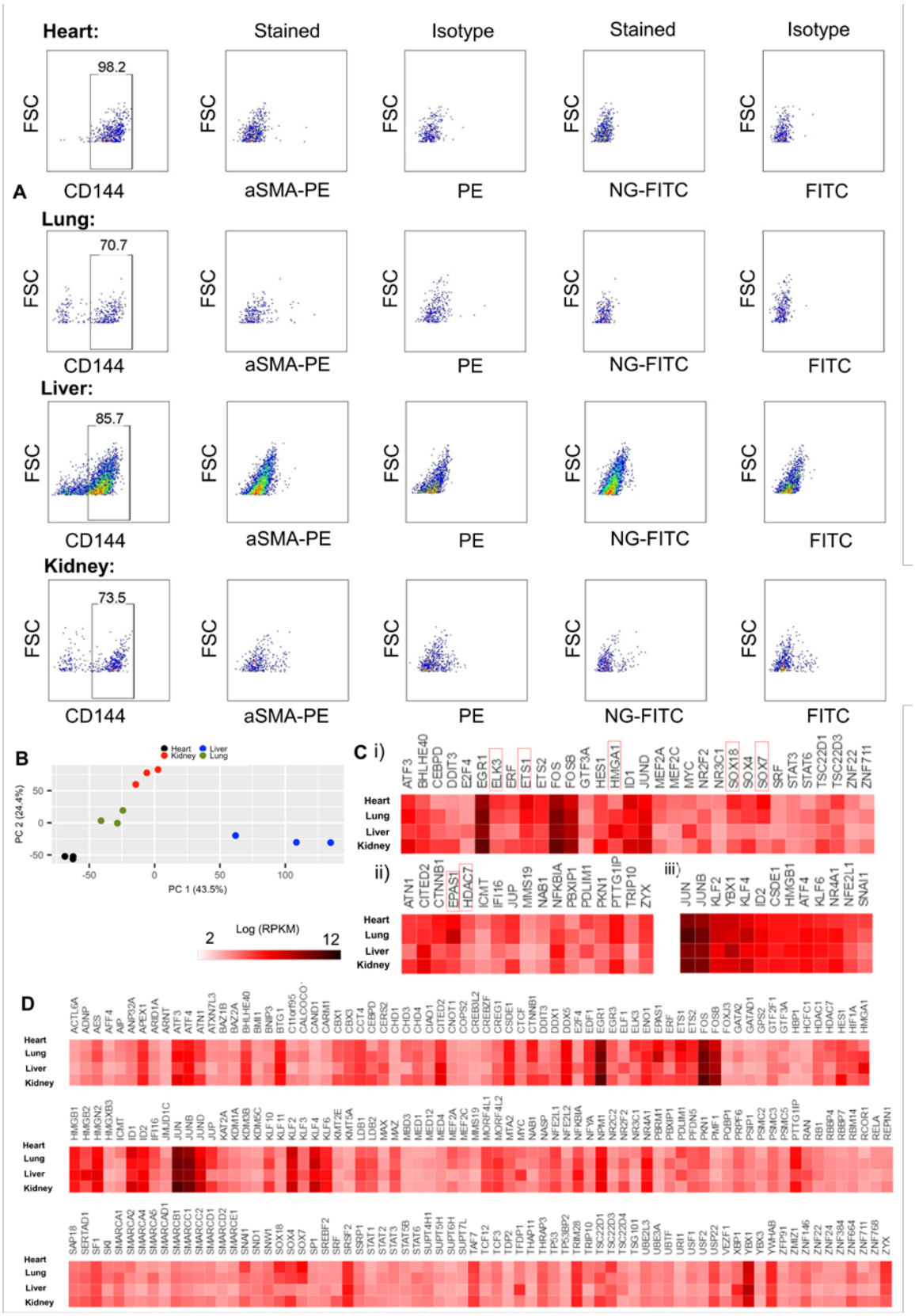
A
Heart:
Stained
Isotype
Stained
Isotype
98.2
FSC
CD144
aSMA-PE
PE
NG-FITC
FITC
Lung:
70.7
Liver:
85.7
Kidney:
73.5
B
Heart
Kidney
Liver
Lung
PC 2 (24.4%)
PC 1 (43.5%)
Log (RPKM)
2
12
C i)
ii)
iii)
ATF3
BHLHE40
CEBPD
DDIT3
E2F4
EGR1
ELK3
ERF
ETS1
ETS2
FOS
FOSB
GTF3A
HES1
HMGA1
ID1
JUND
MEF2A
MEF2C
MYC
NR2F2
NR3C1
SOX18
SOX4
SOX7
SRF
STAT3
STAT6
TSC22D1
TSC22D3
ZNF22
ZNF711
ATN1
CITED2
CTNNB1
EPAS1
HDAC7
ICMT
IFI16
JUP
MMS19
NAB1
NFKBIA
PBXIP1
PDLIM1
PKN1
PTTG1IP
TRIP10
ZYX
JUN
JUNB
KLF2
YBX1
KLF4
ID2
CSDE1
HMGB1
ATF4
KLF6
NR4A1
NFE2L1
SNAI1
Heart
Lung
Liver
Kidney
D
ACTL6A
ADNP
AES
AFF4
AIP
ANP32A
APEX1
ARID1A
ARNT
ATF3
ATF4
ATN1
ATXN7L3
BAZ1B
BAZ2A
BHLHE40
BMI1
BNIP3
BTG1
C11orf95
CALCOCO1
CAND1
CARM1
CBX1
CBX3
CCT4
CEBPD
CERS2
CHD1
CHD3
CHD4
CIAO1
CITED2
CNOT1
COPS2
CREBBP
CREBZF
CREG1
CSDE1
CTCF
CTNNB1
DDIT3
DDX1
DDX5
E2F4
EDF1
EGR1
EGR3
ELF1
ELK3
ENO1
EPAS1
ERF
ETS1
ETS2
FOS
FOSB
FOXJ3
GATA2
GATAD1
GPS2
GTF2F1
GTF3A
HBP1
HCFC1
HDAC1
HDAC7
HES1
HIF1A
HMGA1
HMGB1
HMGB2
HMGN2
HMGXB3
ICMT
ID1
ID2
IFI16
JMJD1C
JUN
JUNB
JUND
JUP
KAT2A
KDM1A
KDM3B
KDM5C
KLF10
KLF11
KLF2
KLF3
KLF4
KLF6
KMT2E
KMT5A
LDB1
LDB2
MAX
MAZ
MED1
MED12
MED4
MEF2A
MEF2C
MMS19
MORF4L1
MORF4L2
MTA2
MYC
NAB1
NASP
NFE2L1
NFE2L2
NFKBIA
NFYA
NPM1
NR2C2
NR2F2
NR3C1
NR4A1
PBRM1
PBXIP1
PDLIM1
PFDN5
PKN1
PMF1
PQBP1
PRPF6
PSIP1
PSMC2
PSMC3
PSMC5
PTTG1IP
RAN
RB1
RBBP4
RBBP7
RBM14
RCOR1
RELA
REPIN1
SAP18
SERTAD1
SF1
SKI
SMARCA1
SMARCA2
SMARCA4
SMARCA5
SMARCAD1
SMARCB1
SMARCC1
SMARCC2
SMARCD1
SMARCD2
SMARCE1
SNAI1
SND1
SNW1
SOX18
SOX4
SOX7
SP1
SREBF2
SRF
SRSF2
SSRP1
STAT1
STAT2
STAT3
STAT5B
STAT6
SUPT4H1
SUPT5H
SUPT6H
SUPT7L
TAF7
TCF12
TCF3
TDP2
TFDP1
THAP11
THRAP3
TP53
TP53BP2
TRIM28
TRIP10
TSC22D1
TSC22D3
TSC22D4
TSG101
UBE2L3
UBE3A
UBTF
URI1
USF1
USF2
USP22
VEZF1
XBP1
YBX1
YBX3
YWHAB
ZFP91
ZMIZ1
ZNF146
ZNF22
ZNF24
ZNF384
ZNF664
ZNF711
ZNF768
ZYX

Fig. S5, related to Fig. 5. Characterization of freshly isolated ECs. A. Representative flow cytometry analysis of freshly isolated ECs via MACS column purification from fetal human heart, lung, liver and kidney stained with antibodies against CD144 (VECad), α-SMA and NG2, in comparison with isotype controls. **B**. 2D principal component analysis of RNA sequencing data shows organ-specific clusters. **C**. Heat map of differentially expressed transcription factors (TFs) (i) and co-factors (ii), and other top expressed TFs (iii) in top 20% expressed transcripts in freshly isolated ECs. C. Heat map of the top 20% expressed TFs and co-factors in freshly isolated heart, lung, liver and kidney ECs. Colormap: log(RPKM).

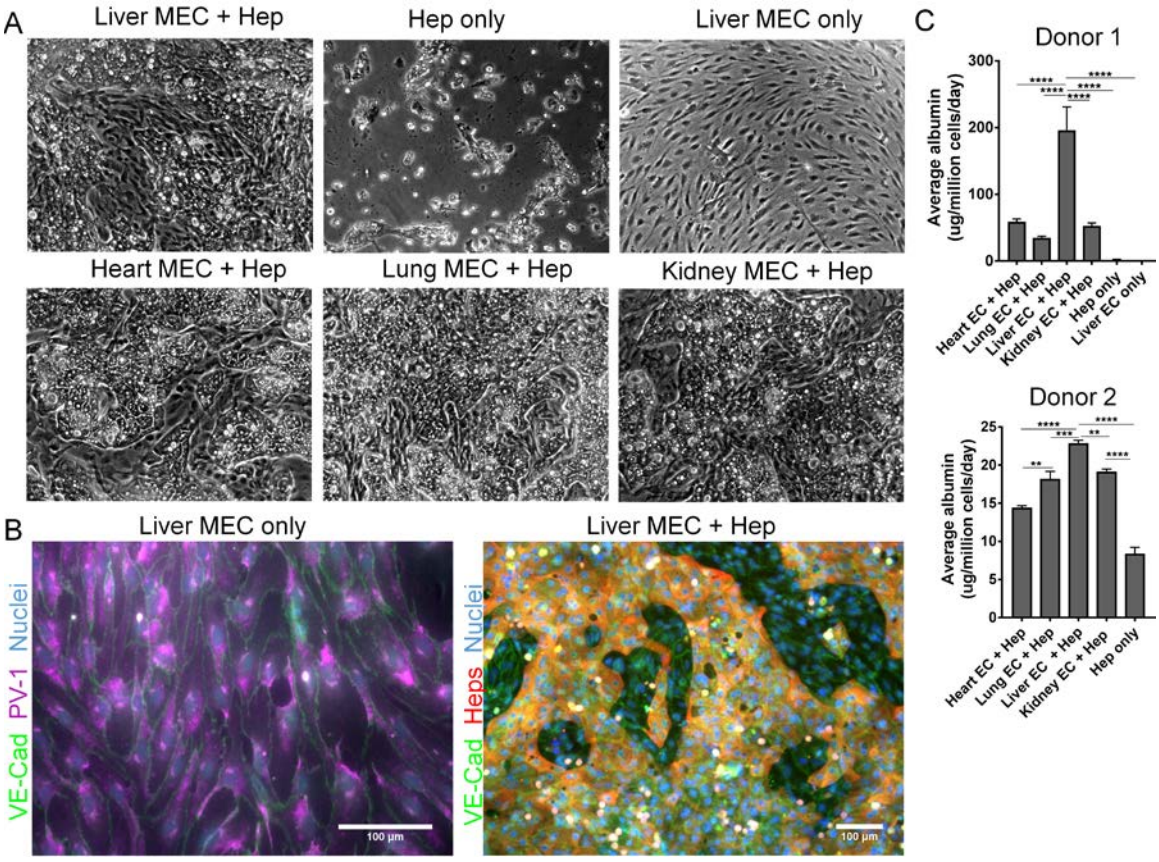

Fig. S6, related to Fig. 6. Human fetal liver ECs superiorly support hepatocytes function. A. Bright field images of 2-D culture after 7 days for EC co-cultured with hepatocytes, hepatocytes alone, or liver ECs alone. B. Immunofluorence image of liver ECs alone and them co-cultured with hepatocytes after 7 days. Hepatocytes were stained with anti-cytokeratin. C. ELISA measurement of albumin production from rat hepatocytes when cultured alone and co-cultured with heart, lung, liver and kidney ECs after 7 days for two donor sets with four replicates in each donor.

Data information: data is presented as mean ± SEM. *p≤0.05, ** p≤0.01, ***p≤0.001, ****p≤0.0001.